Non-Invasive Epicardial Imaging of Human Ventricular Fibrillation

John R Fitz-Clarke, John L Sapp, B Milan Horáček

Dalhousie University, Halifax, NS, Canada

Abstract

The spatial distribution of ECG torso potentials during ventricular fibrillation (VF) might provide useful information about underlying electrical dynamics. We used an inverse solution technique to non-invasively construct images of epicardial activity of human VF.

A 120-lead mapping system was used to record body surface potential maps (BSPM) from eight anesthetized patients during VF induction following implantable defibrillator placement. Epicardial potential maps of VF were derived mathematically by inverse solution using Tikhonov regularization and L-curve method, assuming a homogenous bounded torso.

To assess accuracy, VF was simulated in a large-scale numerical anisotropic heart model incorporating ionic currents. Potential fields were simulated within the torso volume conductor and on the body surface by forward solution to assess the degree of spatial information attenuation. Calculated inverse solution was compared with epicardial activity on the heart model.

Spatial features of VF attenuate with distance from the heart due to the volume conductor; however, the model results demonstrate that inverse solution can resolve epicardial VF patterns to a limited, but potentially useful, degree with larger spatial scales being preserved.

1. Introduction

Ventricular fibrillation (VF) remains a common cause of sudden cardiac death. Survival rates from out-of-hospital cardiac arrest have not improved significantly over the past decade [1]. Only recently have resuscitation algorithms been modified to acknowledge that VF dynamics change with prolonged downtime [2]. Novel approaches are needed to improve resuscitation outcomes. Since ECG signals reflect electrical status of underlying myocardium, better assessment of VF dynamics might lead to improved resuscitation strategies.

Despite VF dynamics being inherently spatiotemporal, the spatial structure of ECG signals on the body surface has received little attention [3]. We sought to study the spatial features of human ECG recordings on the torso surface of patients during induced VF in conjunction with implantable cardioverter-defibrillator (ICD) testing. Computer simulation was then used to explore theoretically the potential utility of spatial analysis. We obtained body surface potential maps (BSPM) of VF, and performed inverse solution to construct epicardial images. These were compared with numerical simulations in a realistic heart and torso model.

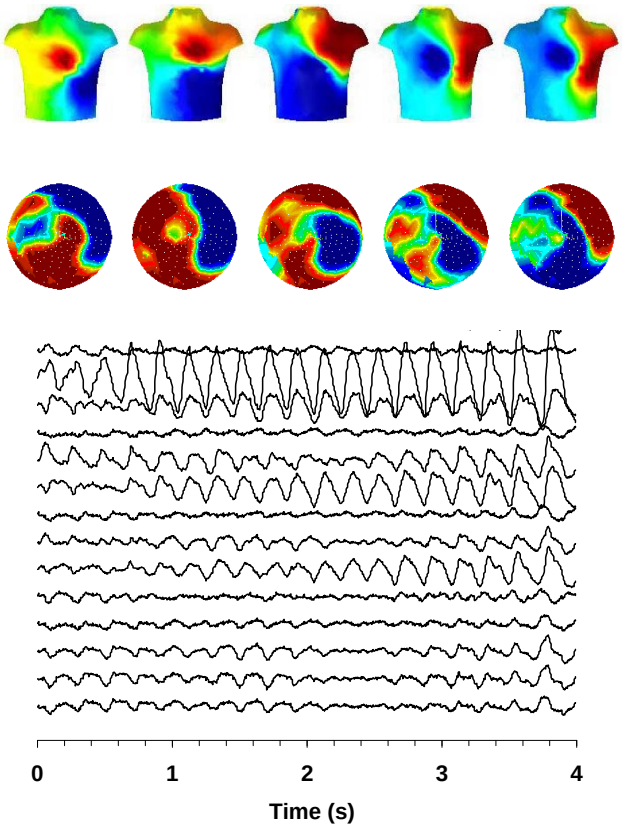

Figure 1. BSPM recordings from a patient in VF, and calculated inverse solution displayed as epicardial maps at 40-ms intervals. Positive voltages are red, and negative voltages are blue. Sample ECG signals showing every eigth lead in the data set are shown below for 4 seconds.

2. Methods

2.1. Patient recordings

Ethics approval was obtained from our institutional review board at the Queen Elizabeth II Health Sciences Centre in Halifax, Canada. Eight patients undergoing ICD implantation were recruited for the study, and each gave informed consent. Custom ECG electrode strips were applied to the anterior and posterior torso surfaces at 120 sites following the Dalhousie convention [4]. Electrodes were not placed at the left subclavian surgical field, nor at sternum and spine sites of adhesive defibrillation pads placed for patient safety. VF was induced by burst pacing of the right ventricular apex after implantation of the ICD under general anesthesia. A 120-lead mapping system was used to record spatial potentials at 2000 Hz per channel over the torso. Recordings were obtained for 5 to 7 seconds until the ICD delivered its internal shock. Signals for each lead were processed off-line to filter out noise and low-frequency baseline wander, and to correct for pacing-induced baseline deviation. Potentials were interpolated at torso regions not covered by electrodes.

2.2. Inverse solution

Torso potentials Φ_B at 352 interpolated sites were mapped onto the epicardial surface Φ_H at each time step. A boundary element method was used to represent torso and epicardial surfaces. Potentials are related $\Phi_B = \mathbf{A}\Phi_H$ through a transfer matrix **A** that embodies the torso volume conductor [5]. This equation is ill-posed, hence epicardial potentials were stabilized using an iterative second-order Tikhonov regularization scheme optimized using the *L-curve* method [6]. Inverse solution was computed at 202 epicardial coordinates to obtain electrocardiographic images of the heart surface. Results were displayed as polar plots.

2.3. Principal component analysis

BSPM data for each patient can be represented as a time-varying linear sum of N fixed orthonormal basis vectors φ_i [7]. Principal component analysis of the space-time data series was performed using the Karhunen-Loeve transform (KLT). This involves constructing the covariance matrix **K** and solving the equation $\mathbf{K}\,\varphi_j = \lambda_j\,\varphi_j$ to obtain the optimal orthogonal eigenvector maps φ_j and corresponding time-dependent eigenvalues λ_j.

2.4 Computational heart model

An anatomically realistic computational human heart model was used to numerically simulate runs of VF. The heart geometry incorporates anisotropic transmural fibre rotation [8]. We used 0.5-mm elements that each contain five time- and voltage-dependent nonlinear ionic currents I_{Na}, I_{Ca}, I_K, I_{KT}, and I_{to} that embody realistic action potential restitution properties, and allow for time-efficient runs of long duration VF [9]. Action potential wave propagation and scroll wave core meander can be visualized within the model.

2.5 Torso conductor

BSPMs from simulated VF runs were computed at the same 352 torso sites as those derived from patient recordings. Torso surface potentials Φ_B were calculated by first assuming the heart to be immersed in an infinite homogeneous volume conductor, and integrating all source dipole contributions from action potentials. The no-flux boundary condition was then imposed on the torso surface through an iterative correction technique incorporating normal vectors at triangular torso elements to obtain the bounded medium solution.

3. Results

Segments of usable data prior to shock ranged from 4.8 to 6.4 sec. Dominant frequencies of ECG signals ranged from 3.10 to 5.08 Hz. BSPMs were seen to have fairly broad areas of positive and negative voltages that moved around the chest with considerable spatial coherence. Epicardial potentials derived by inverse solution from one patient are shown in Figure 1.

Computer simulation of VF with anterior and apical epicardial views is shown in Figure 2 at 40-ms intervals. Resulting BSPMs for this sequence, based on nominal healthy tissue parameters, are shown in Figure 3. Broad areas of opposite voltage polarity are seen to move across the torso surface similar to that seen in patient data. Overall spatiotemporal characteristics are similar to those seen in patient recordings.

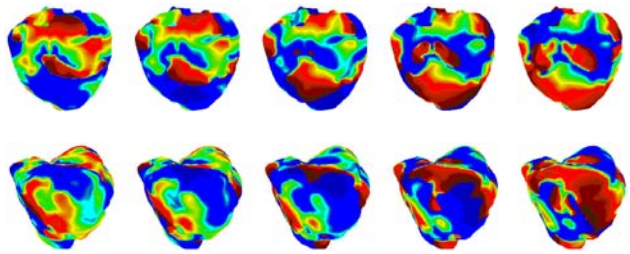

Figure 2. Computer simulation of VF showing anterior (top) and apical (bottom) views at 40-ms intervals using a nominal parameter set for healthy non-ischemic tissue. Action potential waves are red and resting tissue is blue.

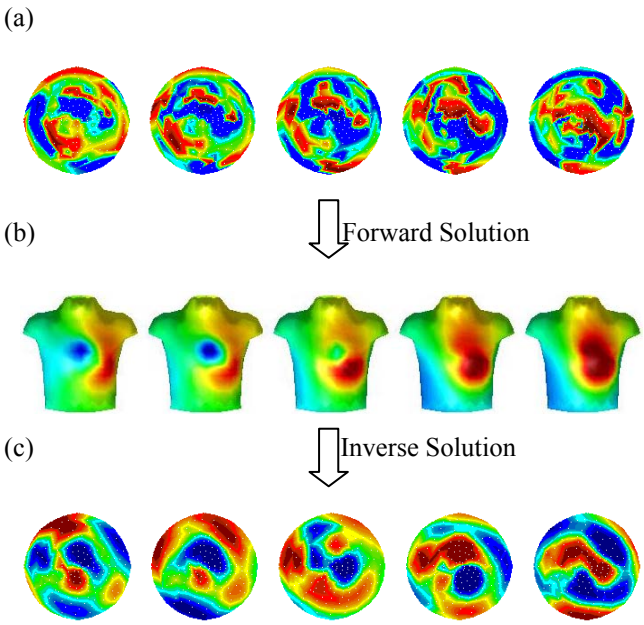

Figure 3. (a) Simulated epicardial potential, (b) derived BSPM sequence, and (c) calculated inverse solution. Note the degree to which calculated epicardial image (bottom) resolves the larger features of the original source (top).

Fine details of VF spatial structure are attenuated with distance away from the heart. Calculated potentials within a cross-section of a cylindrical volume conductor are illustrated in Figure 4 for two sample time steps of VF. In the first image, voltages around the epicardium change slope 12 times around the circumference, yet only 4 such changes in slope are seen on the body surface. In theory, this extracellular field would eventually converge to a single equivalent heart dipole at infinite distance.

Eigenfunction torso maps derived by KLT varied considerably between patients, but each series exhibited a dominant large-voltage dipole pattern and lower-voltage multipolar contributions. We have not attempted to tailor simulations to match specific individual patients. Spatiotemporal data from one KLT-decomposition shown in Figure 5 reveal similar characteristics between one patient and that derived from computer simulation.

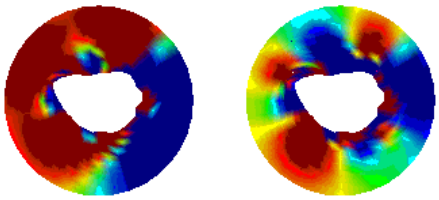

Figure 4. Attentuation of potentials through the volume conductor between the heart and a cylindrical boundary.

4. Discussion

Patient data were restricted to brief segments of induced VF that were non-ischemic. For ethical reasons, VF was not permitted to extend beyond 7 to 10 seconds necessary for ICD charging and shock delivery. Segments clean of pacing and shock artifacts were limited to about 4 to 6 seconds. Signals across leads suggested that torso spatial activity was relatively organized during this period.

BSPMs were constructed from the VF recordings, and inverse solution was used to non-invasively "image" epicardial potentials. Epicardial maps derived by this technique resemble, at least qualitatively, those recorded during open-heart surgery [10] and from perfused explanted myopathic human hearts [11].

Simultaneous recording of both torso and epicardial potentials during human VF is not practical, so validation of the derived epicardial maps poses a challenge. We therefore used the computer model to simulate VF, then calculated the forward solution to generate theoretical BSPMs, and used those torso maps to "back-calculate" inverse solution. Fidelity of epicardial reconstruction could then be compared with the original model heart surface to assess for loss of detail, and get a sense for potential utility of BSPM and imaging of VF.

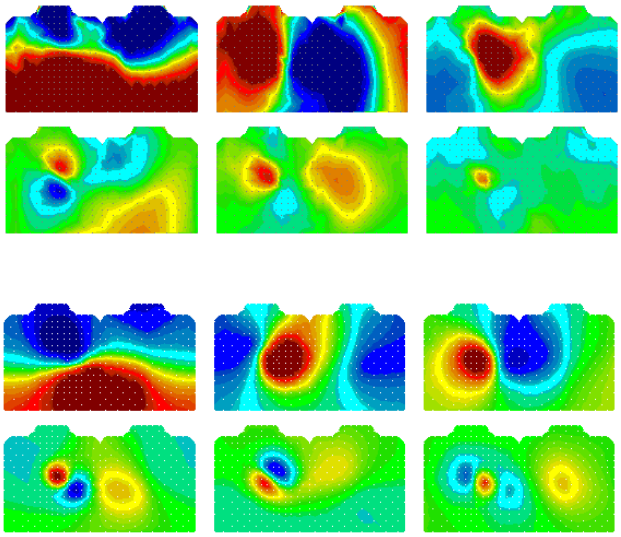

Figure 5. Largest six eigenfunctions of recorded (top) and simulated (bottom) BSPM data over 4 seconds of VF.

Fibrillation is sustained by complex three-dimensional wave propagation within thick ventricular walls. It is not realistic to expect electrical activity to be resolved with high accuracy by an inverse solution that is effectively a two-dimensional compression. Model results, however, demonstrate that inverse solution can be successful in resolving epicardial VF patterns to a limited but

potentially useful degree. The electrical field adjacent to the epicardium due to local action potential wave sources is partially attenuated through the torso volume conductor more distant from the heart, but despite this averaging effect we found that larger spatial scales of epicardial activity are preserved on inverse solution.

Large lead sets are cumbersome in clinical settings, particularly for longer-term monitoring if the patient is at risk for VF. It remains to be determined how reducing the number of torso leads might affect accuracy of derived epicardial maps, yet hopefully still retain useful pattern extraction. Use of a smaller lead set would be more practical in clinical or pre-hospital settings. Use of an appropriate model-based extrapolation to synthesize full BSPMs and carry out similar analysis might be possible. The inverse solution is sensitive to noise in leads, however, and this could impact accuracy of image reconstructions. These issues require further study.

Acknowledgements

The authors thank James Warren for assistance with data analysis. Support for this study was provided by grants from the Canadian Institutes of Health Research, from the Nova Scotia Health Research Foundation, and from Medtronic.

References

[1] Sasson C, Rogers MA, Dahl J, Kellermann AL. Predictors of survival from out-of-hospital cardiac arrest: a systematic review and meta-analysis. Circ Cardiovasc Qual Outcomes 2010; 3:63-81.

[2] American Heart Association guidelines for cardio-pulmonary resuscitation and emergency cardiovascular care. Circulation 2005; 112 (suppl): IV-1–IV-203.

[3] Clayton RH, Murray A, Campbell RWF. Analysis of the body surface ECG measured in independent leads during ventricular fibrillation in humans. Pacing Clin Electrophysiol 1995; 18:1876–81.

[4] Horáček BM, Warren JW, Penney CJ, MacLeod RS, Title LM, Gardner MJ, Feldman CL. Optimal electrocardiographic leads for detecting acute myocardial ischemia. J Electrocardiol 2001; 34(Suppl):97–111.

[5] Horáček BM, Clements JC. The inverse problem of electrocardiography: A solution in terms of single- and double-layer sources on the epicardial surface. Math Biosci 1997; 144: 119–154.

[6] Hansen PC, O'Leary DP. The use of the *L*-curve in the regularization of discrete ill-posed problems. SIAM J Sci Statist Comput 1993; 14:1487–503.

[7] Hubley-Kozey CL, Mitchell LB, et al. Spatial features in body-surface potential maps can identify patients with a history of sustained ventricular tachycardia. Circulation 1995; 92:1825–38.

[8] Hren R. A Realistic Model of Human Ventricular Myocardium: Application to the Study of Ectopic Activation. Ph.D. Thesis. Dalhousie University, 1996.

[9] Fitz-Clarke JR. Spatiotemporal Dynamics of Ventricular Fibrillation in a Three-Dimensional Anisotropic Heart Model. Ph.D. Thesis. Dalhousie University, 2003.

[10] Nash MP, Mourad A, Clayton RH, Sutton PM, Bradley CP, Hayward M, Paterson DJ, Taggart P. Evidence for multiple mechanisms in human ventricular fibrillation. Circulation 2006; 114:536–42.

[11] Massé S, Farid T, Dorian P, Umapathy K, Nair K, Asta J, Ross H, Rao V, Sevaptsidis E, Nanthakumar K. Effect of global ischemia and reperfusion during ventricular fibrillation in myopathic human hearts. Am J Physiol Heart Circ Physiol 2009; 297:H1984-91.

Address for correspondence.

John R. Fitz-Clarke, MD PhD
Department of Physiology and Biophysics
Sir Charles Tupper Medical Building
5859 University Avenue
Dalhousie University
Halifax, Nova Scotia, Canada B3H 4H7
jfitzclarke@eastlink.ca